Environment and Natural Resources Journal

Volume 23
Issue 1
2025

Study of Crystal Structure, Lattice Strain, and Elemental Content of Natural Iron Sand Nanoparticles Synthesized by the Coprecipitation Method

Tulus Na Duma[1], Syahrul Humaidi[1*], Erna Frida[1], Mohd. Mustafa Awang Kechik[2], Muhammadin Hamid[3], Martha Rianna[1], Novita[1], Rahmadhani Banurea[1], Norazimah Mohd Yusof [4], and Nur Jannah Azman[4]

[1]*Postgraduate Program (Physics), FMIPA, Universitas Sumatera Utara, Jl. Bioteknologi No.1, Medan 20155, Indonesia*
[2]*Department of Physics, Faculty of Science, Universiti Putra Malaysia, 43400 UPM Serdang, Selangor, Malaysia*
[3]*Department of Physics, Universitas Sumatera Utara, Jl. Bioteknologi No.1, Medan 20155, Indonesia*
[4]*Faculty of Applied Sciences, Universiti Teknologi MARA, Cawangan Negeri Sembilan, Kampus Kuala Pilah 72000, Kuala Pilah, Negeri Sembilan, Malaysia*

ARTICLE INFO

Received: 13 May 2024
Received in revised: 29 Nov 2024
Accepted: 3 Dec 2024
Published online: 14 Jan 2025
DOI: 10.32526/ennrj/23/20240141

Keywords:
Crystal structure/ Coprecipitation/ Iron sand/ Lattice strain/ Magnetite nanoparticles

*** Corresponding author:**
E-mail: syahrul1@usu.ac.id

ABSTRACT

GRAPHICAL ABSTRACT

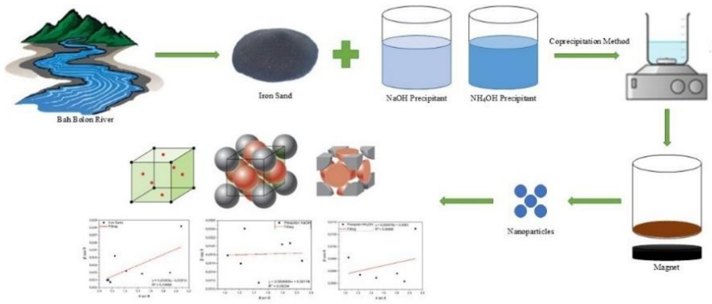

This study was conducted to investigate the synthesis of magnetite nanoparticles from iron sand collected from the Bah Bolon River in Indonesia, using the coprecipitation method with NaOH and NH_4OH as precipitants. The results showed that based on SEM-EDX (scanning electron microscopy coupled with energy-dispersive x-ray spectroscopy) analysis, the Fe content of the raw iron sand, initially at 34.76%, increased to 45.50% following synthesis with NH_4OH, indicating enhanced purity in the final product. SEM observations found average particle sizes of approximately 53 nm for nanoparticles synthesized with NaOH and 20 nm for those synthesized with NH_4OH. X-ray diffraction (XRD) analysis confirmed that the synthesized nanoparticles retain the magnetite (Fe_3O_4) phase with a face-centered cubic (FCC) spinel structure. Crystallite size calculations using the Scherrer equation yielded average crystallite sizes of 80.194 nm for NaOH-synthesized samples and 15.124 nm for NH_4OH-synthesized samples, demonstrating that NH_4OH favors the formation of smaller crystallites. Lattice strain analysis through the Williamson-Hall method showed positive tensile strain values for all samples, indicating structural tension within the crystal lattice. The NH_4OH-synthesized nanoparticles had slightly higher lattice strain, suggesting that synthesis conditions impact both crystallite size and lattice tension. In conclusion, this study demonstrated that NH_4OH was more effective than NaOH in producing high-purity, small-crystallite magnetite nanoparticles from natural iron sand, with potential implications for enhanced material properties.

Citation: Duma TN, Humaidi S, Frida E, Kechik MMA, Hamid M, Rianna M, Novita, Banurea R, Yusof NM, Azman NJ. Study of crystal structure, lattice strain, and elemental content of natural iron sand nanoparticles synthesized by the coprecipitation method. Environ. Nat. Resour. J. 2025;23(1):95-104. (https://doi.org/10.32526/ennrj/23/20240141)

1. INTRODUCTION

Magnetic materials are of significant interest in the field of nanotechnology due to the unique properties, which facilitate application for a variety of advanced purposes. These materials are typically composed of elements such as iron, cobalt, nickel, and alloys, which have intrinsic magnetic behaviors potentially manipulated and enhanced at the nanoscale. Magnetic materials, when synthesized as nanoparticles show characteristics including superparamagnetism, a phenomenon defined as a loss of magnetization in the absence of an external magnetic field, which is advantageous for applications requiring precise control. Additionally, magnetic nanoparticles tend to have higher saturation, facilitating more responsiveness to external magnetic fields. The increased surface area promotes higher reactivity and allows for functionalization, enabling tailored applications in various fields (Díez et al., 2022).

Among magnetic materials, magnetite (Fe_3O_4) has demonstrated particular potential for further development. Fe_3O_4 nanoparticles are widely studied due to the strong magnetic properties, biocompatibility, and versatility in application. The application cuts across a range of fields, including targeted drug delivery, where magnetic properties allow for controlled movement to specific locations in the body. In magnetic resonance imaging (MRI), the nanoparticles act as contrast agents to improve image clarity (Zhang et al., 2022). Other uses include hyperthermia therapy for cancer, where localized heating of tumor cells is achieved through magnetic induction (Wang et al., 2021), and environmental remediation, where magnetic separation can efficiently remove pollutants from water (Fatimah et al., 2023; Tlili et al., 2023).

An important advantage of magnetite is that it can be sourced from nature, providing a potentially sustainable and cost-effective resource for nanoparticle synthesis. Natural deposits of Fe_3O_4 are found in coastal regions, riverbeds, volcanic areas, and green synthesis making it readily available for large-scale production (Elaoud et al., 2024; Novita et al., 2024). Although significant studies have been conducted on Fe_3O_4 nanoparticles synthesized from coastal stands (Yuwanda et al., 2022), data on using river sand as a source are relatively scarce. This gap suggests an opportunity for further investigation into river sands as an alternative natural source of Fe_3O_4, which could expand the availability of sustainable raw materials for magnetite nanoparticle production and open new pathways for applications in nanotechnology.

Various synthesis methods have been used to produce magnetite nanoparticles, each offering unique advantages and influencing the final characteristics. Prominent methods include coprecipitation (Gutierrez et al., 2024; Hamid et al., 2022; Parvathy Namboothiri and Vasundhara, 2023), sol-gel (Hu et al., 2019; Polla et al., 2023), high-energy milling (Calderón Bedoya et al., 2021; Melinia et al., 2022; Rianna et al., 2022), and laser ablation (Al-Salih et al., 2021; Alkallas et al., 2023; Dadashi et al., 2015). Among these methods, coprecipitation is particularly popular due to the simplicity, cost-effectiveness, and ability to yield nanoparticles with controlled size, morphology, and elemental composition. The coprecipitation method entails mixing iron salts in an alkaline medium, allowing for precise manipulation of reaction parameters such as temperature, pH, and the type of precipitating agent used. These parameters play a crucial role in determining the particle size, distribution, and magnetic properties of the resulting nanoparticles, making coprecipitation an adaptable and highly effective method for synthesizing magnetite nanoparticles at both laboratory and industrial scales (Tukan et al., 2023). Although Fe_3O_4 is already present in raw river sand, the coprecipitation method is essential to enhance purity, control particle size, and improve the crystallinity of the synthesized nanoparticles. These improvements are necessary for applications that demand high-purity and consistent particle properties, justifying the use of coprecipitation for refining natural Fe_3O_4 sources.

Studies on magnetite nanoparticle synthesis have shown that the choice of precipitant significantly impacts the characteristics of the final product. Previous studies by Ba-Abbad et al. (2022) explored the effects of different precipitants, such as sodium hydroxide (NaOH) and ammonium hydroxide (NH_4OH), on the morphology and size of magnetite nanoparticles. The results underscore how varying the precipitant can allow fine-tuning of nanoparticle properties, which is essential for tailoring to specific applications. Iron chloride hexahydrate and iron sulfate heptahydrate are commonly used as precursors, reacting with an alkaline solution to form magnetite. However, only a few studies have examined the impact of different precipitants specifically for nanoparticles synthesized from natural iron sand. Examining the effects of different precipitants could provide valuable insights into controlling the structural and magnetic properties of magnetite nanoparticles, particularly those synthesized from natural, sustainable resources.

Understanding the structural characteristics, lattice strain, and elemental composition of magnetite nanoparticles derived from natural iron sand is crucial for optimizing performance across various applications. The crystal structure, for instance, influences magnetic properties and surface reactivity, which are critical for applications such as MRI and targeted drug delivery. Lattice strain, often induced by particle size reduction or imperfections within the crystal lattice, potentially impacts the stability and performance of nanoparticles, making it a key parameter to assess in any synthesis process. Additionally, the elemental composition determines the chemical stability and interaction of nanoparticles with the environment, which is especially relevant in biomedical and environmental applications where compatibility and longevity are essential. By comprehensively characterizing these properties, synthesis methods can be refined to produce nanoparticles with tailored properties, ultimately broadening applicability in scientific and technological fields (Nguyen et al., 2021).

This study aimed to synthesize magnetite nanoparticles from natural iron sand using the coprecipitation method, with a focus on examining the effects of different precipitants, namely NaOH and NH_4OH. A review of existing literature suggests that these precipitants are commonly used for magnetite nanoparticle synthesis, though there are limited studies on the specific effects when applied to natural iron sand sources. This study will investigate how the choice of precipitant influences the crystal structure, lattice strain, and elemental composition of nanoparticles. To achieve this, characterization methods such as x-ray diffraction (XRD) were used to analyze crystal structure and lattice strain while scanning electron microscopy coupled with energy-dispersive x-ray spectroscopy (SEM-EDX) was used to assess particle morphology, size, and elemental content. The results will provide new insights into the potential of natural iron sand as a raw material for high-quality magnetite nanoparticles, paving the way for more sustainable production practices in nanotechnology.

2. METHODOLOGY

2.1 Materials

The natural iron sand used was obtained from the Bah Bolon River, Simalungun Regency of North Sumatra, Indonesia. A previous study focused on analyzing the mineral composition and magnetic characteristics of iron sand (Novita et al., 2023). However, to date, the synthesis of magnetite nanoparticles River has not been undertaken. Further investigation is warranted to examine additional properties of the iron sand after the conversion into magnetite nanoparticles. For the synthesis process, ammonium hydroxide (NH_4OH) at a concentration of 25% (75 mL) and sodium hydroxide (NaOH) at 3 g dissolved in 20 mL of distilled water was used. Additionally, 20 mL of 37% hydrochloric acid (HCl) was utilized.

2.2 Synthesis of magnetite nanoparticles

The synthesis of magnetite nanoparticles was conducted through the coprecipitation method. Initially, 10 g of iron sand were measured and dissolved in 20 mL of 37% HCl. The addition of HCl facilitated the dissolution of iron sand, releasing Fe ions necessary for the formation of magnetite nanoparticles. The acid treatment aided in breaking down the iron sand structure, enhancing the availability of iron for the subsequent reaction steps with NaOH or NH_4OH. This preparation step is crucial for ensuring a homogenous solution of iron ions, which facilitates efficient nanoparticle formation. The dissolution of iron oxides in HCl can be represented by the reactions:

$$\mathrm{Fe_2O_3 + 6HCl \rightarrow 2Fe^{3+} + 3H_2O + 6Cl^-}$$
$$\mathrm{FeO + 2HCl \rightarrow Fe^{2+} + H_2O + 2Cl^-}$$

The solution of iron sand and HCl was stirred at 70°C for 30 min, with agitation maintained at a speed of 500 rpm. Subsequently, a preheated solution of NaOH at 70°C for 10 min was gradually added to the iron sand solution while heating and stirring were continued for an additional hour. This procedure was repeated using 75 mL of 25% NH_4OH solution in place of NaOH. The addition of the base raised the pH, precipitating Fe^{2+} and Fe^{3+} ions as Fe_3O_4 according to the reaction:

$$\mathrm{2Fe^{3+} + Fe^{2+} + 8OH^- \rightarrow Fe_3O_4 + 4H_2O}$$

The use of NaOH and NH_4OH as the precipitant introduced a buffering effect, which stabilizes the pH and supports controlled growth of Fe_3O_4 particles, resulting in nanoparticles with desired purity and size. The synthesized solutions were then allowed to settle, followed by washing of the precipitate with distilled water to eliminate the solvent. Finally, the separated precipitate was dried in an oven at 100°C for 3 h.

2.3 Characterization of magnetite nanoparticles

SEM-EDX analysis, facilitated by Image-J and OriginLab software, was used to examine elemental composition, surface morphology, and particle size. X-ray diffraction (XRD) with CuKα radiation (λ=1.5406 Å) was used to analyze crystal structure and lattice strain, scanning within the range of 20-80° for an angle of 2θ. The crystal size of the synthesized samples was determined using the Scherrer equation (Equation 1), while lattice strain values were assessed using the Williamson-Hall method (Mustapha et al., 2019).

$$d = \frac{K\lambda}{\beta \cos \theta} \quad (1)$$

In the Scherrer equation, K represents Scherrer's constant (K=0.9), β denotes the peak width at half maximum in radians, λ signifies the x-ray wavelength (λ=1.5406 Å), and θ indicates the Bragg diffraction angle measured in radians (Humaidi et al., 2023).

3. RESULTS AND DISCUSSION

3.1 SEM-EDX analysis

SEM-EDX analysis was used to investigate the particle size, surface morphology, and elemental composition of magnetite nanoparticles synthesized from natural iron sand. Figure 1 shows the SEM images at 1,000x magnification, with clear distinctions between the pre- and post-synthesis states of the particles. The raw iron sand (Figure 1(a)) has irregular shapes, asymmetrical protrusions, and a rough surface, likely due to environmental factors including erosion, sediment transport, and deposition in river currents. Following synthesis, the magnetite nanoparticles showed significantly reduced particle size but lacked a fully uniform morphology.

For samples synthesized with NaOH as the precipitant, SEM images showed a moderate reduction in surface roughness, yielding a comparatively smoother texture. In contrast, synthesis with NH_4OH produced smaller particles with reduced surface irregularity and a more porous structure. This morphology may be attributed to NH_4OH which created a more controlled pH environment, resulting

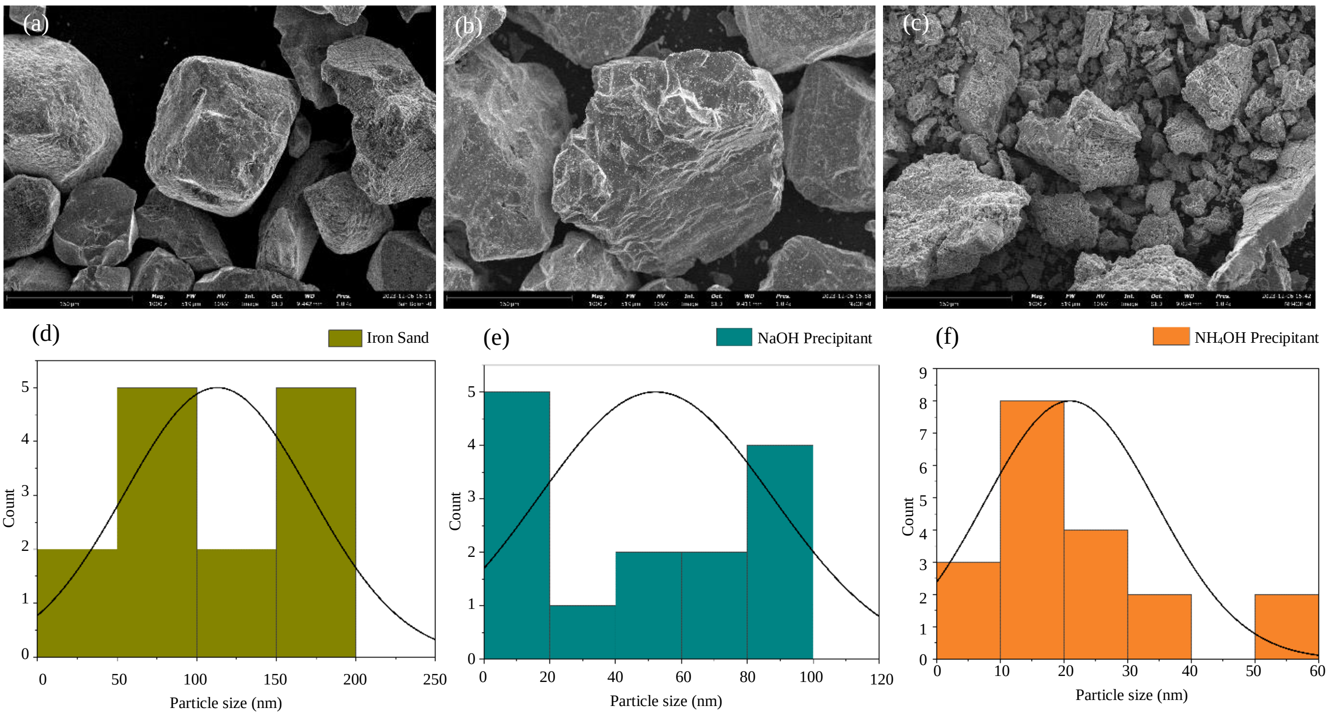

Figure 1. SEM morphology and particle size distribution of natural iron sand and synthesized magnetite nanoparticles (1,000x magnification). SEM images of (a) raw iron sand; (b) iron sand synthesized with NaOH; (c) iron sand synthesized with NH4OH. Histogram of particle size distribution for (d) raw iron sand; predominantly ranging from 100-150 nm; (e) iron sand synthesized with NaOH, with a distribution of 40-80 nm; and (f) iron sand synthesized with NH4OH, exhibiting a narrower range of 20-40 nm.

in slower nucleation and growth, as well as limited particle size. NH_4OH releases ammonia gas during synthesis, which may promote the formation of microvoids within the particles, leading to a porous structure. Although nanoparticle agglomeration is often expected due to high surface energy and particle instability, the SEM images do not show pronounced agglomeration (Figure 1(b) and Figure 1(c)). This may be due to the stabilizing effect of NH_4OH, which supports the formation of dispersed nanoparticles with lower surface energy, reducing visible aggregation despite theoretical tendencies.

Using Image-J and OriginLab software for particle size analysis (Figure 1(d-f)), the average particle size of the iron sand before synthesis was approximately 122 nm. After synthesis, particle size decreased to around 53 nm and 20 nm with NaOH and NH_4OH as precipitants, respectively. NH_4OH yielded smaller particle sizes, attributed to the more acidic reaction environment, which accelerates nanoparticle formation (Mardana et al., 2023). The synthesized particles are larger than those from synthetic precursors namely iron chloride hexahydrate but remain within the nanoscale range, supporting classification as nanoparticles.

EDX analysis was used to examine the elemental composition of the iron sand before and after synthesis into magnetite nanoparticles (Figure 2) (Taufiq et al., 2020). In the natural state, the iron sand sourced from the Bah Bolon River contained 34.76% iron (Fe) and 58.30% oxygen (O), along with trace elements, namely aluminum (Al), silicon (Si), and titanium (Ti), possibly derived from geological and sedimentary processes within the river environment. After synthesis, the Fe content increased to 40.76% and 45.50% with NaOH and NH_4OH as precipitants respectively. This increase indicates successful conversion to magnetite, with NH_4OH demonstrating higher efficiency in promoting Fe incorporation.

The elevated Fe content post-synthesis is consistent with previous studies on natural iron sand sources, which also report increased Fe percentage after processing. Amiruddin and Prayitno (2019) reported a Fe content of 55.33% in iron sand synthesized from Kata Pariaman Beach using the ball milling method. Prasetyowati et al. (2021) observed Fe content up to 60.96% for coastal sand-based magnetite from Kulon Progo Beach. Although the Fe content of magnetite synthesized from Bah Bolon River iron sand is slightly lower than in studies using coastal sources, it still falls within an acceptable range for natural sources, confirming the suitability of river sand for nanoparticle production.

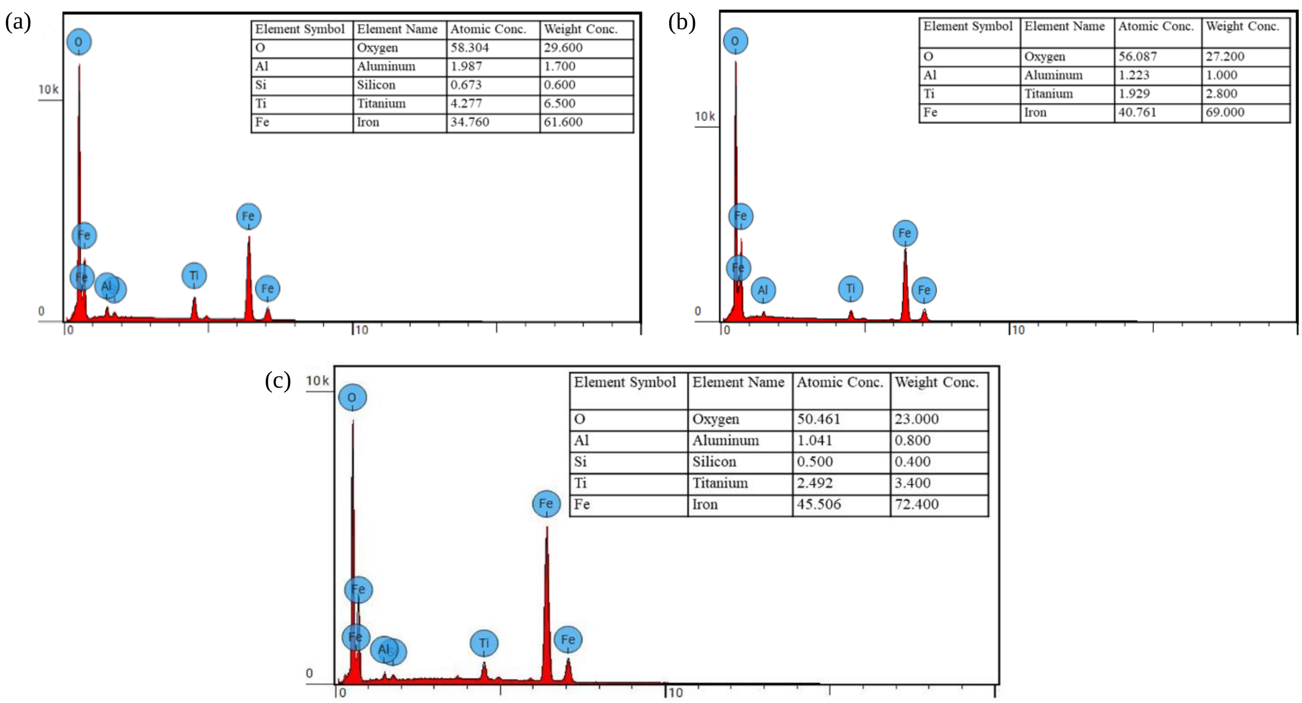

Figure 2. EDX analysis of natural iron sand and synthesized magnetite nanoparticles, displaying elemental composition changes. EDX spectrum of (a) raw iron sand; (b) iron sand synthesized with NaOH; and (c) iron sand synthesized with NH_4OH.

The coprecipitation process used in this study enhanced the Fe content of the final magnetite nanoparticles by facilitating the deposition of ions into a stable Fe_3O_4 crystal structure. The natural iron sand serves as the primary Fe source, containing various iron oxides and other minerals. During the synthesis process, Fe ions are first extracted from the iron sand matrix through dissolution in HCl, which breaks down the mineral structure and releases the ions into solution. The selection of precipitant (NaOH or NH_4OH) plays a critical role. After the addition, the precipitant raises the pH of the acidic Fe ion solution, inducing controlled nucleation and growth of Fe_3O_4 particles through coprecipitation.

In particular, the use of NH_4OH as the precipitant led to a higher Fe content in the nanoparticles compared to NaOH. This effect can be attributed to the greater reactivity and buffering capacity of NH_4OH, which stabilizes the pH more effectively and allows for a more controlled and complete reaction between Fe ions and OH^- ions. Therefore, NH_4OH promotes a faster and more efficient precipitation process, leading to higher Fe incorporation in the magnetite structure. The resulting Fe_3O_4 nanoparticles had a higher Fe density due to the compact magnetite structure formed during precipitation, leading to an increased Fe content compared to the initial iron sand material. Additionally, NH_4OH buffering properties helped limit excessive particle growth, resulting in smaller and more uniform Fe_3O_4 nanoparticles. This controlled environment minimized the presence of other mineral impurities from the iron sand, producing a purer Fe_3O_4 phase with higher Fe content. NH_4OH demonstrated greater efficacy in synthesizing magnetite nanoparticles from natural iron sand by enhancing Fe incorporation, accelerating reaction rates, and producing smaller, more uniformly dispersed particles.

3.2 X-Ray diffraction (XRD) analysis

X-ray diffraction (XRD) analysis provided insight into the crystalline phases, crystallite size, and lattice strain in both the initial iron sand sample and the synthesized magnetite nanoparticles. In this analysis, diffraction peaks were formed from the interaction of X-rays with specific crystal planes within the material, which are identified by the Miller indices (Hamid et al., 2023). Figure 3 shows the diffraction peaks corresponding to the Miller indices. Both the raw iron sand and the synthesized samples showed diffraction peaks corresponding to the Fe_3O_4 (magnetite) phase, suggesting that the material is polycrystalline. Distinct peaks for the magnetite phase appear at (220), (311), (400), (422), (511), and (440) reflections, consistent with the face-centered cubic (FCC) crystal structure in the Fd-3m space group, often referred to as the spinel structure (Sinaga et al., 2023). This phase identification is consistent with the standard reference JCPDS Card No. 19-0629 (Girardet et al., 2022). Additionally, the raw iron sand contains extra peaks corresponding to SiO_2 and α-FeOOH (goethite) phases, identified with Miller indices (111), as per JCPDS Cards No. 46-1045 and No. 29-0713. The presence of SiO_2 is in line with the natural impurities commonly found in iron sands from river sources.

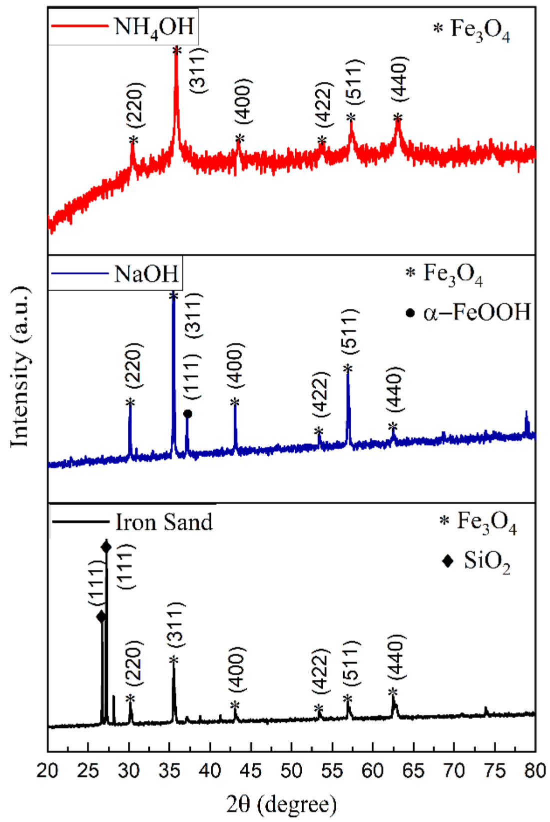

Figure 3. XRD diffraction patterns of natural iron sand and synthesized magnetite nanoparticles. XRD spectra show diffraction peaks corresponding to Fe_3O_4 for both the raw and synthesized samples, indicating a polycrystalline magnetite structure.

For samples synthesized through the coprecipitation method, the XRD pattern for the NaOH-synthesized nanoparticles showed distinct peaks of magnetite along with minor peaks associated with goethite (α-FeOOH). The presence of goethite in this sample suggests that NaOH does not fully reduce iron compounds to the magnetite phase under the synthesis conditions used, potentially leaving behind residual iron oxide impurities. This partial reduction could be attributed to the lower reactivity of NaOH compared to NH_4OH, which might result in a less efficient transformation process. In contrast, the NH_4OH-synthesized sample showed only magnetite peaks, indicating a higher phase purity. This phase purity can be beneficial in applications requiring high magnetic purity, as it minimizes interference from non-magnetic phases including goethite.

The (311) reflection showed the highest peak intensity across all samples, which becomes more pronounced after synthesis. This indicates an alignment preference along the (311) lattice plane in the synthesized magnetite nanoparticles. The diffraction peaks of the NaOH-synthesized nanoparticles are sharper and narrower than those of the NH_4OH-synthesized ones, implying a higher degree of crystallinity and structural regularity in the NaOH sample (Jain et al., 2022). Table 1 shows a comparison of crystallinity percentages and average crystallite sizes for each sample.

Table 1. Comparison of crystallinity and crystal size of each sample

Sample	Crystallinity (%)	Crystallite size (nm)
Iron sand	74.54	90.608
NaOH precipitant	48.94	80.194
NH_4OH precipitant	40.53	15.124

The crystallite size was calculated using the Scherrer formula (Equation 1). The size values obtained were approximately 80.194 nm and 15.124 nm for the sample synthesized using NaOH and NH_4OH respectively. This distinction in crystallite size reflects the influence of precipitant choice on crystal growth, with NH_4OH favoring smaller crystallite formation, possibly due to a more controlled reaction environment. Importantly, this measurement pertains to the average crystallite size rather than the particle, as calculated using the Scherrer equation (Abdel-Mohsen et al., 2022). Crystallite size represents the coherent diffraction domain, which may differ from particle size when particles consist of multiple crystallites.

According to SEM analysis, the average particle sizes are larger than the XRD-determined crystallite sizes, indicating that the nanoparticles may be polycrystalline, consisting of multiple crystallites within a single particle. This observation is especially relevant for magnetite nanoparticles synthesized with NaOH, which show larger crystallite sizes. Polycrystalline particles can impact magnetic properties by reducing the superparamagnetic behavior typically observed in single-crystalline nanoparticles at smaller scales. This suggests that NH_4OH-synthesized nanoparticles, with smaller crystallites and potentially single-domain structures, might show more favorable magnetic properties, such as enhanced superparamagnetic behavior and higher magnetic saturation.

The crystallinity of each sample was analyzed based on the intensity and sharpness of the XRD peaks. The NH_4OH-synthesized sample showed broader peaks, particularly in the (311) reflection, which implies a smaller crystallite size but also may indicate higher lattice strain. This refers to distortions within the crystal lattice, which can be quantified by analyzing peak broadening. In nanostructured materials, lattice strain is often associated with surface defects and structural irregularities that arise during the synthesis process.

Lattice strain can have significant implications for the physical properties of magnetite nanoparticles. To further understand the lattice strain, the Williamson-Hall method was used. Lattice strain, which signifies deformation within the crystal lattice, can arise due to defects, stress, or other imperfections. The Williamson-Hall plot, where $4 \sin\theta$ is plotted against $\beta \cos\theta$, was used to estimate strain (Patel et al., 2024). The lattice strain values calculated were 0.00363 for raw iron sand, 0.0000469 for NaOH-synthesized, and 0.000576 for NH_4OH-synthesized nanoparticles (Figure 4). The positive strain values across samples indicate tensile strain within the lattice. The reduction in lattice strain post-synthesis implies a relaxation in structural tension as the raw iron sand transforms into magnetite nanoparticles. However, the NH_4OH-synthesized sample shows a slightly higher tensile strain than the NaOH-synthesized sample, indicating that NH_4OH promotes a degree of structural strain, possibly due to rapid nanoparticle formation under more acidic conditions.

Higher lattice strain in the NH_4OH-synthesized sample may enhance surface reactivity and catalytic activity, which is advantageous for applications in environmental remediation and biomedical fields where surface interactions are crucial. It also significantly impacts the material mechanical and magnetic properties by increasing stored energy, which can affect mechanical strength, elasticity, and plastic deformation. Additionally, lattice strain introduces localized magnetic anisotropies within the nanoparticles, potentially enhancing the performance in magnetic hyperthermia applications where controlled heating is essential. Strain can further influence properties such as coercivity, magnetoresistance, and atomic diffusion rates, which in turn impact chemical reactivity. Therefore, the choice of precipitant not only affects crystallite size but also plays a key role in determining the structural and functional characteristics of the synthesized nanoparticles.

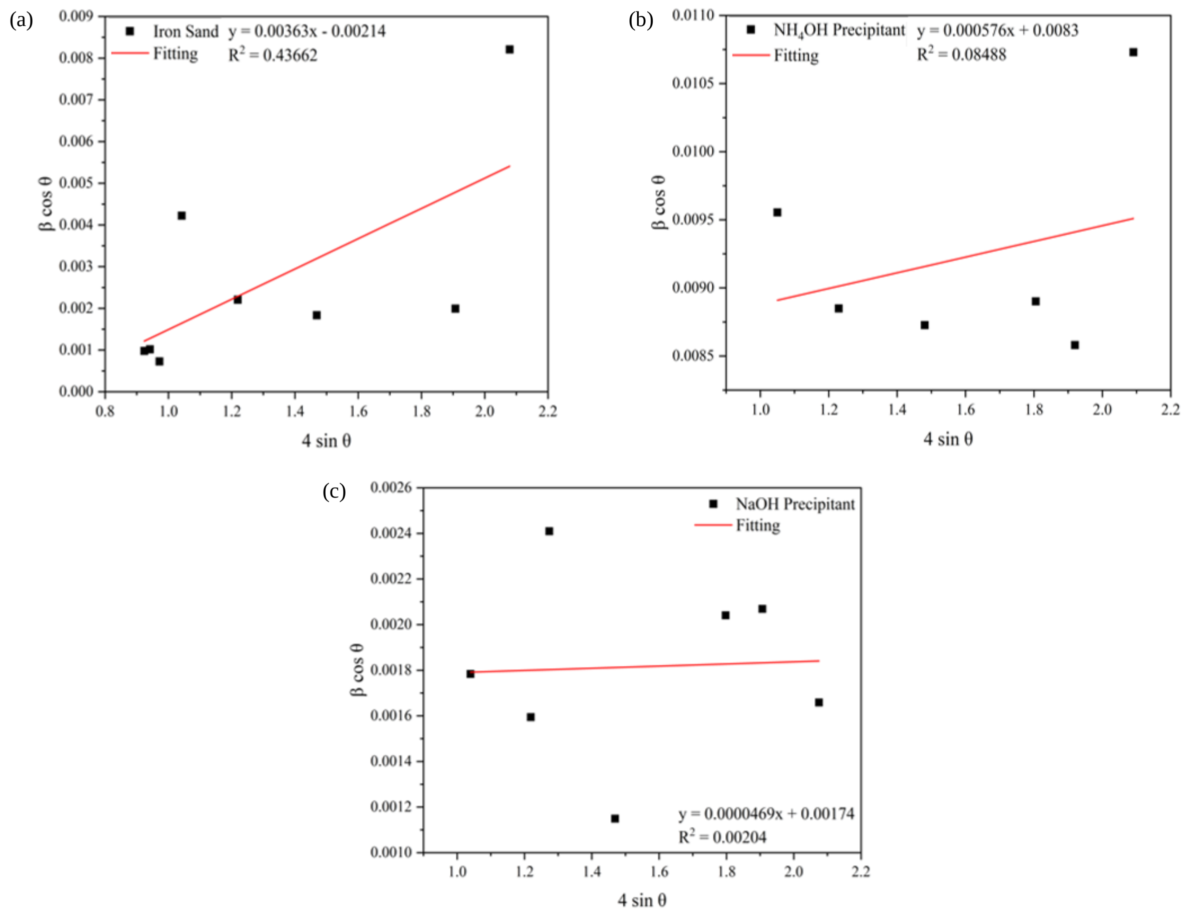

Figure 4. W-H Plot (Williamson-Hall Plot) for estimating lattice strain of natural iron sand and synthesized magnetite nanoparticles. Raw iron sand (a) exhibits the hightest strain due to impurities and distortions. NH_4OH-synthesized magnetite (b) shows reduced strain; while NaOH-synthesized magnetite (c) has the lowest strain. All samples display positive lattice strain, indicating tensile strain within the crystal lattice.

4. CONCLUSION

In conclusion, the successful synthesis of magnetite nanoparticles from natural iron sand was achieved through the coprecipitation method using two distinct precipitants, namely NaOH and NH_4OH. The results showed that the choice of precipitant significantly impacted the shape and size of the resulting magnetite nanoparticles. NH_4OH precipitant demonstrated higher performance in synthesizing magnetite nanoparticles from natural iron sand compared to NaOH, as evidenced by an increase in Fe content, accelerated reaction kinetics, and production of smaller particle sizes. Moreover, the NH_4OH precipitant yielded purer magnetite nanoparticles with a more regular crystal structure and higher crystallinity relative to NaOH. Iron sand samples synthesized with NH_4OH precipitant also showed a higher level of tensile strain. The selection of precipitants in the synthesis process of magnetite nanoparticles from natural iron sand significantly influenced the crystal structure, lattice strain, and elemental composition.

ACKNOWLEDGEMENTS

The authors are grateful to the Postgraduate Program of Physics, FMIPA, Universitas Sumatera Utara, Indonesia, and the Department of Physics, FMIPA, Universitas Sumatera Utara, Indonesia for the support and encouragement to complete this project through the facilities provided and PMDSU Program Batch VII Year of 2023.

REFERENCES

Abdel-Mohsen LH, Lafta SH, Hashim MS. Comparing the role of NaOH and NH_4OH on structural and magnetic properties of spinel ba ferrite synthesized by autocombustion method. Journal of Physics: Conference Series 2022;2322:Article No. 012081.

Al-Salih M, Samsudin S, Arshad SS. Synthesis and characterizations iron oxide carbon nanotubes nanocomposite by laser ablation for anti-microbial applications. Journal of Genetic Engineering and Biotechnology 2021;19(1):Article No. 76.

Alkallas FH, Alghamdi SM, Rashed EA, Trabelsi ABG, Nafee SS, Elsharkawy WB, et al. Nanocomposite Fe_3O_4-MWCNTs based on femtosecond pulsed laser ablation for catalytic degradation. Diamond and Related Materials 2023;140(PA):Article No. 110445.

Amiruddin E, Prayitno A. The synthesis of magnetic nanoparticles from naturaliron sand of Kata Beach Pariaman West Sumatera using ball milling method as environmental material. MATEC Web of Conferences 2019;276:Article No. 06014.

Ba-Abbad MM, Benamour A, Ewis D, Mohammad AW, Mahmoudi E. Synthesis of Fe_3O_4 nanoparticles with different shapes through a co-precipitation method and their application. Journal of the Minerals, Metals and Materials Society 2022;74(9):3531-9.

Calderón Bedoya PA, Botta PM, Bercoff PG, Fanovich MA. Magnetic iron oxides nanoparticles obtained by mechanochemical reactions from different solid precursors. Journal of Alloys and Compounds 2021;860:Article No. 157892

Dadashi S, Poursalehi R, Delavari H. Structural and optical properties of pure iron and iron oxide nanoparticles prepared via pulsed Nd:YAG laser ablation in liquid. Procedia Materials Science 2015;11:722-6.

Díez AG, Rincón-Iglesias M, Lanceros-Méndez S, Reguera J, Lizundia E. Multicomponent magnetic nanoparticle engineering: The role of structure-property relationship in advanced applications. Materials Today Chemistry 2022;26: Article No. 101220.

Elaoud A, Mechi A, Tlili H, Ferhi M, Hassen H Ben. Green synthesis and characterization of magnetite nanoparticles using eucalyptus globulus leaves for water treatment and agronomic valorization. Environmental Monitoring and Assessment 2024;196(9):Article No. 786.

Fatimah S, Juharni J, Wahyuni ASH. Green synthesis of Fe_3O_4 nanoparticles based on natural sand as methylene blue degradation by electrocoagulation method. Positron 2023;13(1):86-94.

Girardet T, Venturini P, Martinez H, Dupin JC, Cleymand F, Fleutot S. Spinel magnetic iron oxide nanoparticles: Properties, synthesis and washing methods. Applied Sciences 2022;12(16):Article No. 8127.

Gutierrez FV, Lima IS, De Falco A, Ereias BM, Baffa O, Diego de Abreu Lima C, et al. The effect of temperature on the synthesis of magnetite nanoparticles by the coprecipitation method. Heliyon 2024;10(4):e25781.

Hamid M, Rianna M, Rangkuti WR, Sembiring T, Sebayang P. Study and characterization RGO/Fe_3O_4 in microstructure and magnetic properties. South African Journal of Chemical Engineering 2022;42:280-2.

Hamid M, Susilawati, Amaturrahim SA, Dalimunthe IB, Daulay A. Synthesis of magnetic activated carbon-supported cobalt(II) chloride derived from pecan shell (*Aleurites Moluccana*) with co-precipitation method as the electrode in supercapacitors. Materials Science for Energy Technologies 2023;6:429-36.

Hu P, Chang T, Chen WJ, Deng J, Li SL, Zuo YG, et al. Temperature effects on magnetic properties of Fe_3O_4 nanoparticles synthesized by the sol-gel explosion-assisted method. Journal of Alloys and Compounds 2019;773:605-11.

Humaidi S, Hamid M, Wijoyo H. Study and characterization of $BaFe_{12}O_{19}$-PVDF materials prepared by co-precipitation for supercapacitor electrodes applications. Authorea 2023; DOI: 10.22541/au.169887066.61389194/v1.

Jain R, Kumar S, Meena SK. Precipitating agent (NaOH and NH_4OH) dependent magnetic properties of cobalt ferrite nanoparticles. AIP Advances 2022;12:Article No. 095109.

Mardana IBP, Lutfiyah YN, Yasa P, Widiantara GKA. Synthesis and characterization of magnetite Fe_3O_4 nanoparticles from natural iron sand in Gelar River. Indonesian Physical Review 2023;6(1):114-23.

Melinia LA, Puspita E, Naibaho M, Ramlan R, Ginting M. Analysis of natural iron sand from Musi River, South Sumatra. Journal of Scientific Research 2022;24(3):Article No. 122.

Mustapha S, Ndamitso MM, Abdulkareem AS, Tijani JO, Shuaib DT, Mohammed AK, et al. Comparative study of crystallite size using williamson-hall and debye-scherrer plots for ZnO nanoparticles. Advances in Natural Sciences: Nanoscience and Nanotechnology 2019;10(4):Article No. 045013.

Nguyen MD, Tran H-V, Xu S, Lee TR. Fe_3O_4 nanoparticles : structures, synthesis, magnetic properties, surface functionalization, and emerging applications. Applied Sciences 2021;11:Article No. 11301.

Novita N, Naibaho M, Puspita E, Ramlan R, Ginting M, Humaidi S. Analysis of mineral content and magnetic properties of iron sand of Bah Bolon Simalungun River, North Sumetera. Asian Journal of Engineering, Social and Health 2023;2(12):1633-9.

Novita, Ramlan, Naibaho M, Ginting M, Humaidi S, Duma TN. Fe_2O_3 review: Nanostructure, synthesis methods, and applications. International Journal of Social Service and Research 2024;04(02):539-59.

Parvathy Namboothiri PM, Vasundhara M. Synthesis and characterization of nano-hematite. Materials Today: Proceedings 2023;92:1459-63.

Patel K, Patel A, Jethwa VP, Patel H, Solanki GK. X-Ray diffraction analysis of orthorhombic SnSe nanoparticles by

Williamson-Hall, Halder-Wagner and Size-Strain plot methods. Chemical Physics Impact 2024;8:Article No. 100547.

Polla MB, Nicolini JL, Venturini J, da Cas Viegas A, Zen Vasconcellos MA, Montedo ORK, et al. Low-temperature sol-gel synthesis of magnetite superparamagnetic nanoparticles: influence of heat treatment and citrate-nitrate equivalence ratio. Ceramics International 2023;49(5):7322-32.

Prasetyowati R, Widiawati D, Swastika PE, Ariswan A, Warsono W. Synthesis and characterization of magnetite (Fe_3O_4) nanoparticles based on iron sands at Glagah Beach Kulon Progo with coprecipitation methods at various NH_4OH concentrations. Journal of Basic Science 2021;10(2):57-61.

Rianna M, Hamid M, Handayani F, Sebayang AMS, Rangkuti WR, Situmorang M, et al. Study and characterization of Fe_3O_4 synthesized from natural iron sand in Sumatera Utara. Journal of Aceh Physics Society 2022;11(2):45-8.

Sinaga JEE, Budianto G, Pritama VL, Suhendra. Particle Size and Lattice Strain Effect on the Optical Constants of Fe_3O_4 Nanoparticles. Indonesian Physical Review 2023;6(1):114-23.

Taufiq A, Nikmah A, Hidayat A, Sunaryono S, Mufti N, Hidayat N, et al. Synthesis of magnetite/silica nanocomposites from natural sand to create a drug delivery vehicle. Heliyon 2020;6(4):e03784.

Tlili H, Elaoud A, Asses N, Horchani-naifer K, Ferhi M, Goya GF, et al. Reduction of oxidizable pollutants in waste water from the Wadi El Bey River Basin using magnetic nanoparticles as removal agents. Magnetoche 2023;9(6):Article No. 157.

Tukan DN, Rosmainar L, Kustomo K, Rasidah R. A review: optimum conditions for magnetite synthesis (Fe_3O_4). Journal of Scientific Periodicals of Science and Applied Chemistry 2023;17(2):Article No. 15.

Wang W, Li F, Li S, Hu Y, Xu M, Zhang Y, et al. M2 macrophage-targeted iron oxide nanoparticles for magnetic resonance image-guided magnetic hyperthermia therapy. Journal of Materials Science and Technology 2021;81:77-87.

Yuwanda AN, Rahmayuni R, Visgun DA, Rahmi A, Rifai H, Dwiridal L. Characterization of magnetic minerals of iron sand Pasia Nan Tigo Padang Beach using X-Ray diffraction (XRD). Indonesian Journal of Applied Physics 2022;12(1):35-47.

Zhang W, Zhang Z, Lou S, Chang Z, Wen B, Zhang T. Hyaluronic acid-stabilized Fe_3O_4 nanoparticles for promoting In vivo magnetic resonance imaging of tumors. Frontiers in Pharmacology 2022;13:Article No. 918819.